

Investigation of Encapsulated Selenium Nanoparticles with PLGA Polymers Against MCF-7 and HBL Cell Lines

Haider Hamzah Al-Shreefy¹, Estabraq Al-Wasiti¹, Mohammed J. Al-Awady^{2,3}✉

¹ Department of Biochemistry, College of Medicine, Al Nahrain University, Baghdad, Iraq

² Department of Biotechnology, College of Biotechnology, Al Qasim Green University, Babylon, Iraq

³ Department of Chemistry, Faculty of Science, University of Western Ontario, London, Canada

✉ Corresponding author. E-mail: M.Awady@biotech.uoqasim.edu.iq

Received: Mar. 16, 2022; **Revised:** Nov. 15, 2022; **Accepted:** Mar. 31, 2023

Citation: H.H. Al-Shreefy, E. Al-Wasiti, M.J. J Al-Awady. Investigation of encapsulated selenium nanoparticles with PLGA polymers against MCF-7 and HBL cell lines. *Nano Biomedicine and Engineering*, 2023.

<http://doi.org/10.26599/NBE.2023.9290013>

Abstract

As cancer-related deaths continue to rise, developments in nanotechnology have emerged as a feasible option for finding successful treatments targeting cancerous cells while avoiding all of the drawbacks of traditional drugs. Selenium nanoparticles (SeNPs) have been reported to exhibit an inhibitory effect on cancerous cells. The aim of the present study was to use the drug delivery systems poly(lactic-co-glycolic acid) (PLGA) and poly(lactic-co-glycolic acid-poly(ethylene glycol)-folic acid (PLGA-PEG-FA) to encapsulate SeNPs and investigate their antineoplastic effects against two cell line types (MCF-7 as a positive folate receptor and HBL as a negative folate receptor) by exploiting overexpression features in some types of cancer cells to ensure delivery of drug molecules at high dosages toward targeted cells and circumvent normal cells/tissues. SeNPs were chemically synthesized and characterized with dynamic light scattering (DLS) and transmission electronic microscopy (TEM). The cytotoxicity of both nanomaterials was evaluated against MCF-7 and HBL cells by using the methyl thiazolyl tetrazolium (MTT) assay which showed a high cytotoxic effect against MCF-7 cells with a lesser effect against HBL cells. Additionally, an apoptosis assay was also performed by using acridine orange/ethidium bromide dual staining, and the antioxidant effect was also investigated by using the 2,2-diphenyl-1-picrylhydrazyl (DPPH) colorimetric method with high antioxidant potential for both formulations. They showed nonhemolytic activity on human red blood cells. This work could be considered promising for pharmaceutical formulation.

Keywords: selenium nanoparticles (SeNPs); vitamin E TPGS; drug delivery system; poly(lactic-co-glycolic acid) (PLGA); MCF-7 breast cancer cells

Introduction

Polymeric nanoparticles (PNPs) are constructed and designed to be compatible with human body (so-called biocompatible) and can be degradable in various physiological conditions into nontoxic molecules (called biodegradable). Polymers range in

size from 10 nm to 1 μ m where the drug is dissolved, encapsulated, entrapped, and in some cases attached to a matrix of these polymers [1]. The formulation of a therapeutic agent with PNPs can improve drug stability, solubility, permeability, and thus therapeutic effects as well as decrease their side effects, with degradation intervals that can be reached for months,

depending on the needs and physicochemical properties of the polymers and the nature of the loaded material [2]. PNPs offer protection of drug against chemical degradation with physical stabilization, making them have high enhanced permeability and retention (EPR) effects due to their size with high loading capacity [3, 4].

This field is growing rapidly and has an important role in a many sectors such as environmental technology, electronics, biotechnology, pollution control, and medicine. PNPs are promising vehicles for drug delivery by simple manipulation to fabricate carriers with the aim of delivering the drugs to a particular target tissue or organ. PNPs transport drugs, proteins, small peptides, vaccines, and DNA to target cells and organs, due to their nanoscale which encourages permeation effectively via cell membranes and stability in the blood stream. Biodegradable polymers are very appropriate materials for the manufacture of countless and varied molecular designs that can be integrated into exclusive nanoparticle constructs with many potential medical applications [1, 5, 6].

There are two types of biodegradable polymers used for nanodrug delivery: natural and synthetic polymers. Natural polymers also called biopolymers are directly obtained from natural origins such as animals, plants, algae, and bacteria [7]. PNPs are solid systems classified into two categories nanospheres and nanocapsules, depending on the type of polymer used, the localization of the active agent, and the production method [8]. Poly(lactic-co-glycolic acid) (PLGA) polymers are approved by the Food and Drug Administration (FDA) and European Medicine Agency (EMA) for medical use in various drug delivery systems for humans [9]. Poly(lactic-co-glycolic acid-poly(ethylene glycol)-folic acid (PLGA-PEG-FA) is a PLGA polymer with surface modification by folic acid as a cancer-targeting ligand and using PEG as a linker that covalently links the targeting molecule (folate) and the therapeutic payload (Se-TPGS, TPGS is tocopherol polyethylene glycol 1000 succinate); these linkers can be cleavable under different conditions, such as acidity conditions at the tumor site, labile to enzymes such as esterase and specific proteases at the tumor site susceptible to cleavage by exogenous chemicals or enzymes given intravenously on-demand at the desired time [10]. Folate decorated PLGA can be synthesized by

PEGylation of PLGA polymer based on a process that involves a covalent conjugation of active PEG to a polymeric or therapeutic delivery system [11]. The method of PEGylation can be extended to different nanoformulations, polymers, liposomes, peptides, small molecule drugs, antibodies, and nucleotides [12]. In addition to the biocompatible and biodegradable nature of PEG molecules, they have other advantages of using PEG in nanodrug formulations to prolong the time of nanomaterials in blood circulation without release and tend to accumulate at leaky vasculature sites, carrying the entrapped medicine with them and decreasing polymeric nanoparticle harmfulness [13–15]. Furthermore, the PEG surface group can be functionalized with different molecules or ligands, especially those that possess high affinity to cell receptors to increase targeting approaches to increase intracellular uptake for therapeutic efficacy or diagnostic approaches through the protective transportation of the medicine particularly to cancerous cells/tissues [16].

Malignant cells possess excessive cell proliferation, so they require more folic acid (acting as a coenzyme for pyrimidine and purine biosynthesis). Cancer cells overexpress the folate receptor (FR) to take in folic acid. A higher degree of FR expression was detected on the surface of cancer cells in a solid tumor, and the density of FR appears to be increased compared to normal tissues at an advanced cancer stages. Because of its location, density, distribution pattern, increased folic acid absorption capacity, and folic acid specificity, FR is a viable target for nanotherapeutics [17]. Cancer cells express 500 times more folate receptors than normal cells. As a result, the high affinity of folic acid for folate receptors offers exceptional prospects for the specific targeting and delivery of nanoparticles to cancer cells [18].

In the current work, vitamin E TPGS stabilized selenium nanoparticles (SeNPs) were synthesized by chemical reduction with ascorbic acid, which were then encapsulated separately with PLGA and PLGA-PEG-FA polymers to form SeNPs-TPGS-PLGA nanoparticles and SeNPs-TPGS-PEG-FA NPs via emulsion evaporation technique as seen in Fig. 1. The particle size distribution, zeta potential (ZP), and transmission electron microscope of each formulation were investigated and found to be (110 ± 20) nm and (-12 ± 8) mV for SeNPs-TPGS-PLGA and

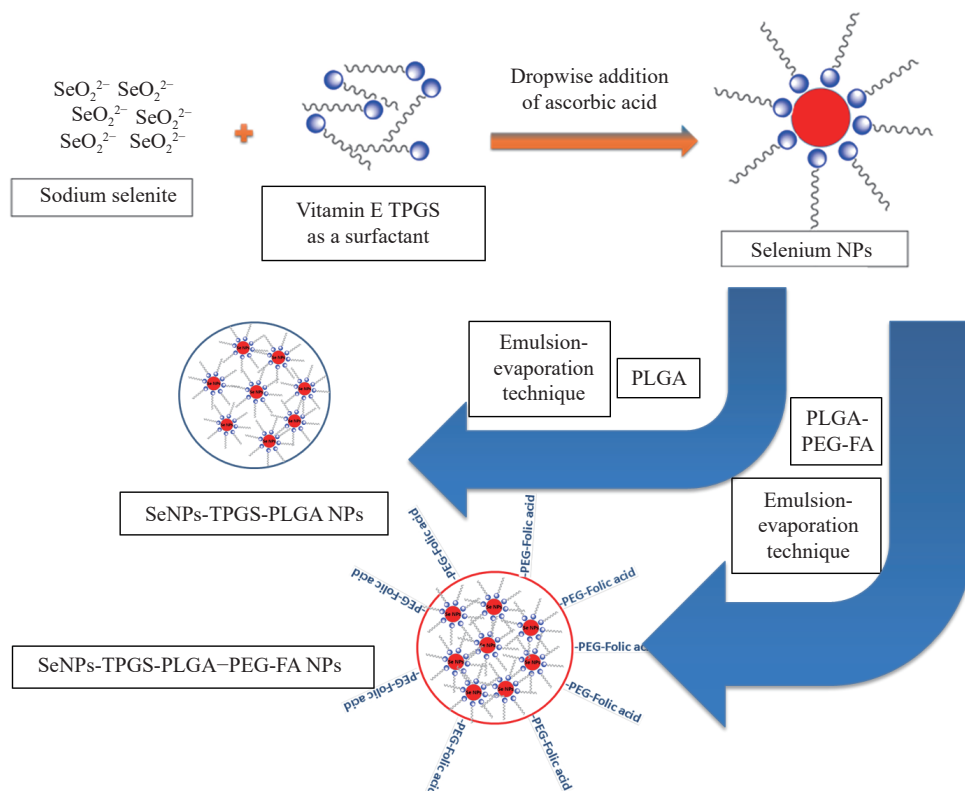


Fig. 1 Flowgram of synthesis of vitamin E TPGS stabilized selenium NPs encapsulated into PLGA polymer and PLGA-PEG-FA polymer to form SeNPs-TPGS-PLGA NPs and SeNPs-TPGS-PLGA-PEG-FA NPs.

(116 ± 30) nm and (-15 ± 10) mV for SeNPs-TPGS-PEG-FA NPs, as well as the morphology of PLGA-based nanoparticles was spherical in shape with minimum aggregation in the shelf life. The cytotoxicity of PLGA and folate decorated PLGA nanoparticles has appeared profound toxic effect towards MCF-7 cancerous cells in comparison with that for HBL-100 cells. In addition to that, they showed more apoptotic effects with high antioxidant activity on MCF-7 as well as significant hemocompatibility in case of incubation with red blood cells (RBC). This formulation could be promising for biomedical applications as chemotherapy for the treatment of breast cancer.

Experimental

Materials

Sodium selenite, dichloromethane (DCM), ethanol alcohol, and polyvinyl alcohol (PVA) were purchased from HIMEDIA (India), and PLGA (lactide:glycolide = 50:50, molecular weight 30–75 kDa) was purchased from Corbion (the Netherlands). PLGA-PEG-FA was purchased from Bioman (China). Trypsin/EDTA, RPMI 1640 media, and fetal bovine serum (FBS) were purchased from Capricorn. L-ascorbic acid was

purchased from Alpha Chemika. TPGS was purchased from Antares. Acridine orange (AO), ethidium bromide (EtBr), and methyl thiazolyl tetrazolium (MTT) were purchased from Bio-World. Dimethyl sulfoxide (DMSO) was also purchased from Santa Cruz Biotechnology. Penicillin streptomycin was purchased from Invitrogen. Hanks' balanced salt solution (HBSS) and 2,2-diphenyl-1-picrylhydrazyl (DPPH) were purchased from Sigma-Aldrich. MCF-7 and HBL cells were purchased from American Type Culture Collection (ATCC).

Synthesis and purification of selenium nanoparticles

5.0 mmol/L of sodium selenite (Na_2SeO_3) solution was prepared by dissolving 216 mg sodium selenite of in 250 mL of deionized water. 0.3 mol/L ascorbic acid as a reducing agent solution was freshly prepared by dissolving 2.64 g of its crystals in 50 mL of deionized water. 0.02 g of vitamin E TPGS was dissolved in 500 mL of deionized water. 500 mL of vitamin E TPGS solution was mixed with 5 mL of sodium selenite solution under a magnetic stirrer at 600 r/min. Then, 5 mL of ascorbic acid was added dropwise with stirring reduced to 300 rpm, and 10 mL of deionized water was added to a final volume of 25 mL. The solution was increasingly converted from

colorless to intense orange-red, and the reaction was allowed to proceed for a total of one day at room temperature to ensure a high yield of SeNPs with high polydispersity index. Se-TPGS NPs could be purified by using a dialysis bag with a 12 000 relative molecular mass cut-off, to remove excess TPGS and ascorbic acid, against deionized water for at least 1 h .

Encapsulation of SeNPs into PLGA polymer

The SeNPs encapsulated with PLGA synthetic polymer were prepared through emulsion solvent evaporation with some modifications. In brief, 20 mg of PLGA polymer was dissolved in 2 mL of DCM as the organic phase and then mix with 10 mL of Se-TPGS NP solution as aqueous phase; this mixture of two solutions was directly shaken vigorously by a sonication probe for 1 min under ice bath until the solution became miscible and the appearance of the solution was altered distinctly to milky-white. The new solution was kept in an expelled place for evaporating and completely removing the organic solvent DCM in the environment with stirring at 25 °C for 3 h. The final product was centrifuged three times at 8 000 r/min for 30 min. The obtained precipitate was resuspended in distilled water repeatedly by centrifugation and was dried to obtain dry composite powder. The prepared SeNPs-PLGA nanocomposites were stored under anhydrous and dark conditions at 4 °C [19].

Encapsulation of SeNPs into PLGA-PEG-FA polymer

SeNPs encapsulated with PLGA-PEG-FA polymer were prepared by using a double emulsification procedure by organic solvent evaporation. Briefly, a mixture of 5 mL of SeNPs as the aqueous phase and 25 mg of PLGA-PEG-FA polymer was dissolved in 10 mL of DCM and emulsified using an ice bath with a sonication for 1 min. Then, 20 mL of 3% PVA was added, and a second emulsification at 90% amplitude in an ice bath was performed for 1 min. The organic solvent was evaporated under magnetic stirring at room temperature for 6 h. Next, a 2-min centrifugation cycle at 2 000 r/min was employed, and the supernatant was collected. The supernatant was washed three times with centrifugation cycles at 15 000 r/min for 10 min, the supernatant was discarded, and the pellet was resuspended in deionized water [20].

Characterization

Dynamic light scattering (DLS) and zeta potential measurement

The hydrodynamic particle size and zeta potential measurement of SeNPs-TPGS-PLGA NPs and SeNPs-TPGS-PLGA-PEG-FA NPs were measured using Zetasizer Nano ZS (Malvern, UK) according to DLS technique.

Transmission electron microscopy (TEM)

Colloidal suspensions (20 µL) of nanoformulations were placed onto 400 mesh carbon-copper TEM grid support film and allowed to dry at room temperature. The sample analysis was performed on a transmission electron microscope (JEOL-JEM-2100 F, Japan) with an accelerating voltage of 80 kV.

Cytotoxicity assay *in vitro*

The breast cell line MCF-7 (surface positive folate receptor) and HBL (negative folate receptor) were used to evaluate the cytotoxicity of encapsulated formulas (Se-TPGS-PLGA and Se-TPGS-PLGA-PEG-FA), and every type of cell was maintained in Roswell Park Memorial Institute (RPMI-1640) media supplemented with 10% FBS, with a mixture of penicillin (100 units/mL) and streptomycin (100 µg/mL). The cells were reseeded into trypsin-EDTA and incubated in a humidified incubator (Cypress Diagnostics, Belgium) with 5% CO₂ at 37 °C [21, 22]. Both cell lines (MCF-7 and HBL) were seeded at 10⁴ cells/well into 96-well plates. After 24 h, the cells were treated with the tested compound at different concentrations. RPMI-1640 medium without any treatment was used as a control. Cell viability was measured after 72 h of treatment by removing the medium, adding 28 µL of 2 mg/mL solution of MTT, and incubating the cells for 2.5 h at 37 °C. After removing the MTT solution, the crystals remaining in the wells were solubilized by the addition of 130 µL of DMSO followed by incubation at 37 °C for 15 min with shaking [23, 24]. The absorbance was determined on a microplate reader (Microtiter reader, Gennex Lab, USA) at 492 nm; the assay was performed in triplicate. The inhibition rate of cell growth (the percentage of cytotoxicity) was calculated by [25]

$$\text{Inhibition rate} = \frac{\text{OD}_{\text{control}} - \text{OD}_{\text{sample}}}{\text{OD}_{\text{control}} - \text{OD}_{\text{blank}}} \times 100\% \quad (1)$$

where OD_{blank} , OD_{control} , and OD_{sample} are the optical density of the blank, control, and sample, respectively.

AO/EtBr viability assay

To prepare stock solution of AO/EtBr double stains, 15 mg of acridine orange and 50 mg of ethidium bromide were dissolved in 1 mL of ethanol alcohol. This solution was then completed to 50 mL by adding distilled water, and then divided into 1-mL aliquot and kept in deep freeze ($-20\text{ }^{\circ}\text{C}$) for at least 3 months. To prepare working solution of AO/EtBr dual staining, thawing of 1.0-mL aliquot was thawed in 100 mL of HBSS, which will stay stable for 1 month [26]. The cell lines (2.0×10^6 cells/mL) were cultured and incubated for 24 h and then tested against Se-TPGS-PLGA and Se-TPGS-PLGA-PEG-FA. The cells were harvested by trypsinization, centrifuged to collect the cell pellet washed twice,

and resuspended in cold phosphate buffer, then stained with 100 μL of AO/EtBr solution then was mixed smoothly for 2 min before visualization by fluorescence microscopy and the sample directly assessed [27].

Antioxidant activity of SeNPs and polymeric formulations

The scavenging capacity of the Se-TPGS-PLGA and Se-TPGS-PLGA-PEG-FA formulations was evaluated using a stable DPPH assay. A total of 500 μL of the two formulations was added to 500 μL of DPPH solution, and the volume was brought up to 2 mL using absolute ethanol alcohol with ascorbic acid as a reference material. The absorbance of each compound was measured at 517 nm [28]. The free radical scavenging test (DPPH) was performed in triplicates measurement and the results were presented as the mean \pm SD. DPPH radical scavenging activity was calculated by

$$\text{Scavenging activity} = \frac{\text{Absorbance of control} - \text{absorbance of samples}}{\text{Absorbance of control}} \times 100\% \quad (2)$$

Hemolytic activity on RBCs

Blood samples (2.5 mL) were obtained from healthy volunteers in EDTA tubes, and the blood was centrifuged for 1 min at 4 000 r/min to precipitate the red blood cells in the pellet. The supernatant was removed and washed with normal saline solution 0.9% NaCl three times. The tested nanomaterials were added to blood samples at a concentration of 10 $\mu\text{g}/\text{mL}$. After 60 min of incubation at $37\text{ }^{\circ}\text{C}$, the fluorescence intensity of RBCs was examined using a fluorescence microscope [29].

Statistical analysis

The experiments were repeated separately at least three times. Statistical analysis of *t*-test was performed using GraphPad Prism version 8.0.0. A *P*-value of ≤ 0.05 was considered statistically significant.

Results and Discussion

Encapsulation of SeNPs with PLGA polymers

Coating or wrapping of synthesized nanoparticles with biocompatible and biodegradable PLGA and PLGA-PEG-FA polymers is shown in Figs. 2(b) and 2(c). The encapsulation process preserved the spherical shape of SeNPs as stated in Fig. 2(a), by

enclosing the nanoparticles as well as protecting and stabilizing them for extended time in colloidal solution. Using PLGA for encapsulation of SeNPs becomes stable for at least three months [30]. Polymers can be modified with different targeting moieties (such as folate), which affects the biological responsivity by altering both the pharmacodynamics and pharmacokinetic profile of the payload [31]. The size of PLGA polymeric nanoparticles can be enlarged by increasing the concentration of PLGA and selecting a high polymer relative molecular mass [32].

DLS

DLS is a noninvasive method for determining the hydrodynamic size of nanoparticles in suspension based upon the random movement of particles due to collisions initiated by bombardment with the solvent molecules that surround the nanoparticles by measuring the speed of particles undergoing Brownian motion [33]. The hydrodynamic size of the particles was measured by DLS analysis, as depicted in Fig. 2. This study revealed that the particle size obtained from the highly dispersed colloidal solution was expressed as Z_{average} (nm) for Se-TPGS = (75 ± 15) nm, Se-TPGS-PLGA = (110 ± 20) nm, and Se-TPGS-PLGA-PEG-FA = (116 ± 30) nm as shown in Table 1. All these results were measured three

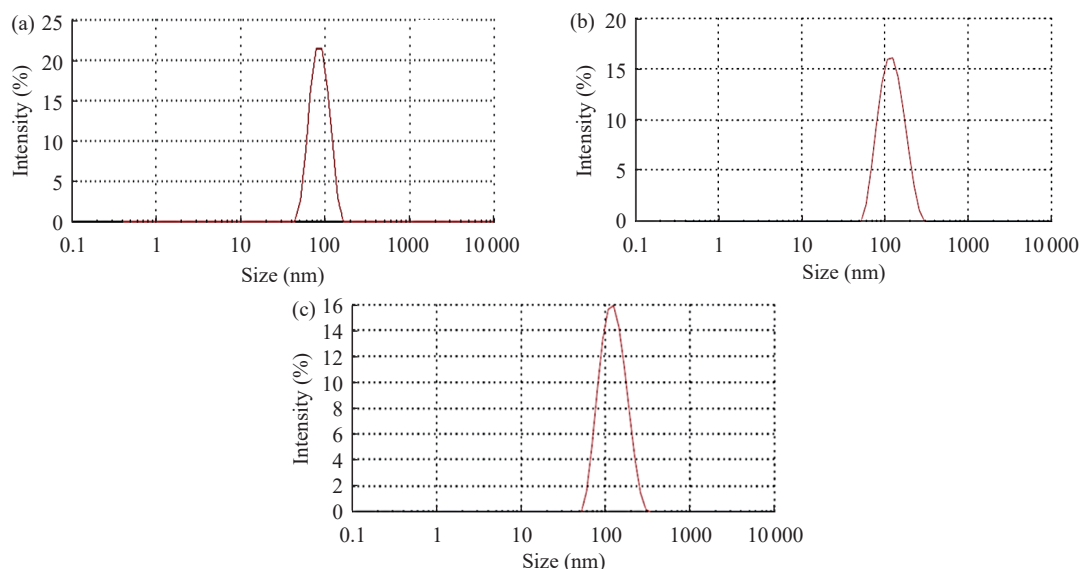


Fig. 2 Particle size distribution of (a) SeNPs synthesized by chemical reduction with ascorbic acid in the presence of vitamin E TPGS as a surfactant, (b) the synthesized SeNPs-vitamin E TPGS encapsulated into PLGA polymer in the form of SeNPs-TPGS-PLGA NPs, and (c) the synthesized SeNPs-vitamin E TPGS encapsulated into PLGA-PEG-FA polymer in the form of SeNPs-TPGS-PLGA-PEG-FA NPs.

Table 1 Average particle diameter and zeta potential measurement of nanoformulations

Nanoformulation	Z_{average} (nm)	Zeta potential (mV)	PDI
Se-TPGS NPs	75 ± 15	-20 ± 10	0.143
Se-TPGS-PLGA NPs	110 ± 20	-12 ± 8	0.149
Se-TPGS-PLGA-PEG-FA NPs	116 ± 30	-15 ± 10	0.154

times per run at room temperature and reproduced every three months and found to be completely stable in the shelf life with slightly aggregation.

The determination of particle size is one of the fundamental steps for prospective nanoparticle applications. The main benefit of nanoparticles, particularly metallic-based nanoparticles, is that they can be achieved with controlled size. The nanoparticle size influences their biodistribution, cellular uptake, and excretion by the body [34]. The size of synthesized nanoparticles for medical purposes plays a crucial role in their extended blood circulation. Usually, nanoparticles less than 100 nm in size permit a longer half-life *in vivo* and reduced hepatic filtration [35]. The reduction in particle size from 5 000 to 200 nm increases the surface area of the particle by a factor of 25 in addition to increasing solubility [36]. The size distribution of SeNPs determines their anticancer activity [37]. The α -tocopherol-ascorbic acid encapsulated with PLGA nanoparticles offered a size of 90–126 nm, whereas using sorbitan monooleate gives polymeric nanoparticles with sizes of 155–216 nm [38]. PLGA is biocompatible, sustained drug release and

possesses the ability to act as a carrier for diverse materials and nanoparticles; thus, many drug formulations have been developed for cancer therapy by means of phenomena in tumor tissue termed the increased EPR effect, which allows these drug-loaded nanoparticles to penetrate through the tumor vasculature, delivering their payload into the cells and thereby boosting their therapeutic impact [39].

The ZP values are shown in Table 1 which indicates the higher stability of the monodispersed suspension of the nanoparticles as described in Fig. 3. The zeta potential of the synthesized SeNPs indicated that they were relatively negatively charged in nature. ZP is a predictor factor for colloidal solution stability. This parameter shows the degree of repulsion between the charged nanoparticles in the dispersion. High ZP values indicate highly charged NPs, which prevents aggregation of these particles especially in the presence of stabilizers, because of increasing electric repulsion. If the ZP is low, attraction overcomes repulsion, and it is likely that the mixture forms coagulates [40, 41]. The surface properties of nanoparticles such as surface charge have a considerable effect in addition to the morphological

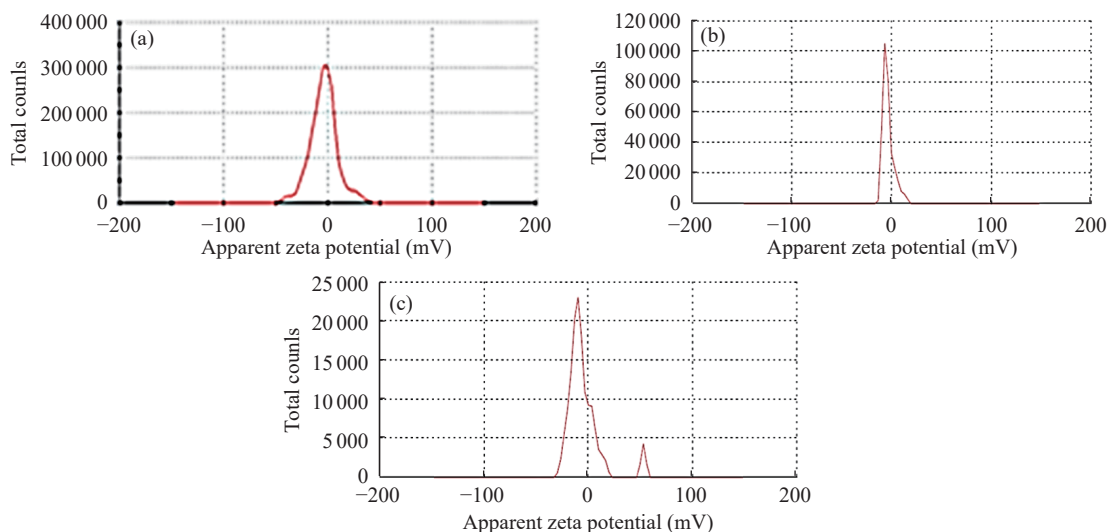


Fig. 3 Zeta potential measurement of (a) SeNPs synthesized by chemical reduction with ascorbic acid in the presence of vitamin E TPGS as a surfactant, (b) the synthesized SeNPs-vitamin E TPGS encapsulated into PLGA polymer in the form of SeNPs-TPGS-PLGA NPs, and (c) the synthesized SeNPs-vitamin E TPGS encapsulated into PLGA-PEG-FA polymer in the form of SeNPs-TPGS-PLGA-PEG-FA NPs.

properties. The surface charge of nanoparticles is an extrinsic property or system-dependent, i.e., changed with their milieu (pH and biological molecules) that interacts with nanoparticles [34]. Nanoparticles possessing a neutral or somewhat negative surface charge are favored to extend the circulation time [42]. The finding of negatively charged zeta potential values for all colloidal suspensions. Table 1 refers to the presence of electrostatic repulsion forces or is sometimes expressed as electrostatic stabilization between nanoparticle components. Although selenium in the nano formula does not possess any charge in the elemental valence state (Se^0), the measured surface charges can be attributed to the adsorption of ions and/or charged molecules that present in the SeNP milieu, either during synthesis or after assembly [43].

TEM

TEM is an analytical apparatus that provides morphological, crystalline structural, and chemical information even for a single nanoparticle [44]. As shown in the TEM images in Fig. 4, the chemical approach for synthesizing SeNPs was spherical. The images of SeNPs loaded separately into PLGA polymer and PLGA-PEG-FA polymer (see Figs. 4(b) and 4(c)) show the framing and protecting the nanoparticles, which are called nanospheres and have a solid polymeric structure with a spherical shape. The increase in the PLGA concentration extended the period required for drug release in case of nanoparticles loading drug molecules before the

encapsulation process [45]. The TEM technique is broadly used and is a skillful tool to differentiate between nanospheres and nanocapsules, in addition to being able to determine the width of the nanocapsule wall [46].

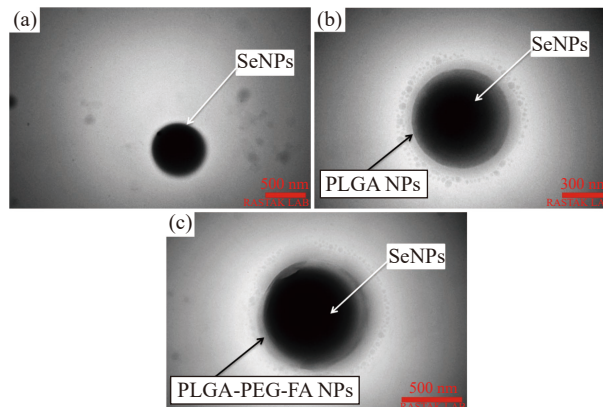


Fig. 4 TEM images of (a) SeNPs synthesized by chemical reduction with ascorbic acid in the presence of vitamin E TPGS as a surfactant, (b) the synthesized SeNPs-vitamin E TPGS encapsulated into PLGA polymer in the form of SeNPs-TPGS-PLGA NPs, and (c) the synthesized SeNPs-vitamin E TPGS encapsulated into PLGA-PEG-FA polymer in the form of SeNPs-TPGS-PLGA-PEG-FA NPs.

MTT cell viability assays

The results showed highly significant cytotoxic activity of Se-TPGS-PLGA and Se-TPGS-PLGA-PEG-FA against human cancer cell lines as shown in Figs. 5(a) and 5(b), in which the half-maximal inhibitory concentration (IC_{50}) is a measure of the effectiveness of a new formulation in inhibiting

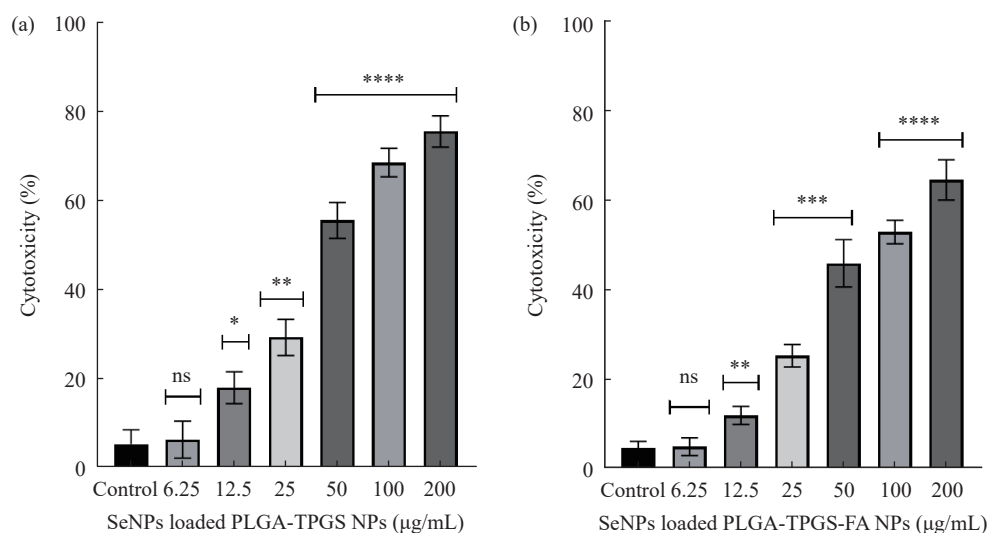


Fig. 5 MTT cytotoxicity assay of MCF7 cells upon incubation with (a) SeNPs synthesized by chemical reduction with ascorbic acid in the presence of vitamin E TPGS as a surfactant and encapsulated into PLGA polymer in the form of SeNPs-TPGS-PLGA NPs and (b) the synthesized SeNPs-vitamin E TPGS encapsulated into PLGA-PEG-FA polymer in the form of SeNPs-TPGS-PLGA-PEG-FA NPs. Statistical analysis of MTT cytotoxic assay of 100 and 200 µg/mL SeNPs-TPGS-PLGA-PEG NPs as well as 100 and 200 µg/mL SeNPs-TPGS-PLGA-PEG-FA NPs in comparison with the control sample. All results were performed in triplicate and repeated three times and achieved statistically using GraphPad Prism 8.0 where non-significant (ns) $P > 0.05$, $*P \leq 0.05$, $**P \leq 0.01$, $***P \leq 0.001$, and $****P \leq 0.0001$.

biological/biochemical functions. The IC_{50} value for Se-TPGS PLGA formula equals to 42.15 µg/mL, whereas for Se-TPGS-PLGA-PEG-FA equals to 48.31 µg/mL, and there was no substantial effect against normal HBL cells as stated in Figs. 6(a) and 6(b). This outcome is attributed to synergistic effect of selenium and vitamin E TPGS. SeNPs (stabilized with red algae polysaccharide) can infiltrate into brain cells that have poor permeability such as glioma parenchyma which represents a major challenge for anti-glioblastoma drug delivery. These nanoparticles were non-cytotoxic towards normal glial brain cells but showed high antineoplastic activity towards

malignant glioma (U-87 MG) cells with an $IC_{50} = 9.1$ µmol/L, and 27.6 µmol/L for the glioma cell line (C6) [47]. Li et al. [48] applied a different strategy by conjugating folic acid with the TPGS molecule (TPGS-FA) as a nanocarrier for delivering nitidine drugs to induce apoptosis in a hepatocellular cell line (Huh7) that overexpresses folate receptors. Shahverdi et al. [49] functionalized SeNPs directly with folic acid as a capping agent via ascorbic acid reduction of selenium dioxide and investigated their anticancer effect *in vivo* (mouse model) and *in vitro* against 4T1 as a positive folate receptor derived from mammary mouse gland tissue.

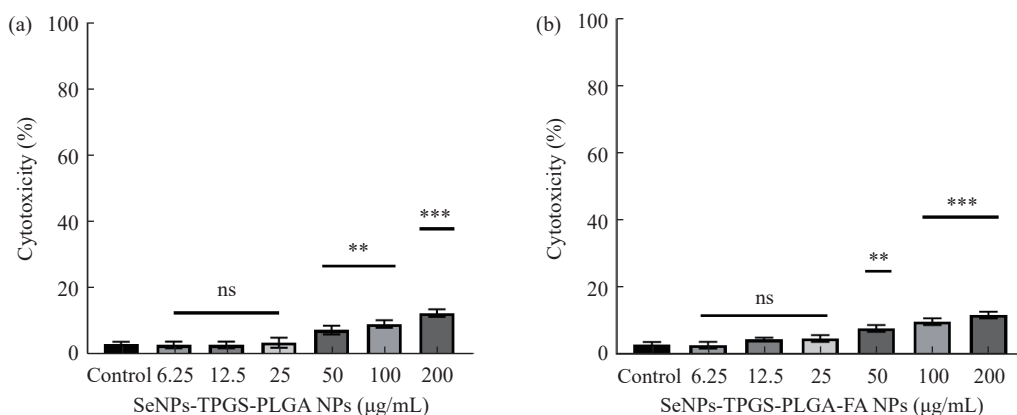


Fig. 6 MTT cytotoxicity assay of HBL-100 cells upon incubation with (a) SeNPs synthesized by chemical reduction with ascorbic acid in the presence of vitamin E TPGS as a surfactant and encapsulated into PLGA polymer in the form of SeNPs-TPGS-PLGA NPs and (b) the synthesized SeNPs-vitamin E TPGS encapsulated into PLGA-PEG-FA polymer in the form of SeNPs-TPGS-PLGA-PEG-FA NPs. All results were performed in triplicate and repeated three times and achieved statistically using GraphPad Prism 8.0 where non-significant (ns) $P > 0.05$, $*P \leq 0.05$, $**P \leq 0.01$, $***P \leq 0.001$, and $****P \leq 0.0001$.

Cell morphological analysis

When comparing untreated (alive cells) images under an inverted microscope, it was observed that the morphology of MCF-7 and HBL cells cultured in RPMI-1640 media had a standard morphology and attached to the surface as illustrated in Figs. 7(a) and 8(a). After treatment with Se-TPGS-PLGA and Se-TPGS-PLGA-PEG-FA at IC_{50} concentrations, MCF-7 cells lost their attachment and deteriorated towards a rounded structure and floated in the culture medium as described in Figs. 7(b) and 7(c), while the HBL showed no change in their morphology, no floating, and reached for confluence 95%–100% (Figs. 8(b) and 8(c)).

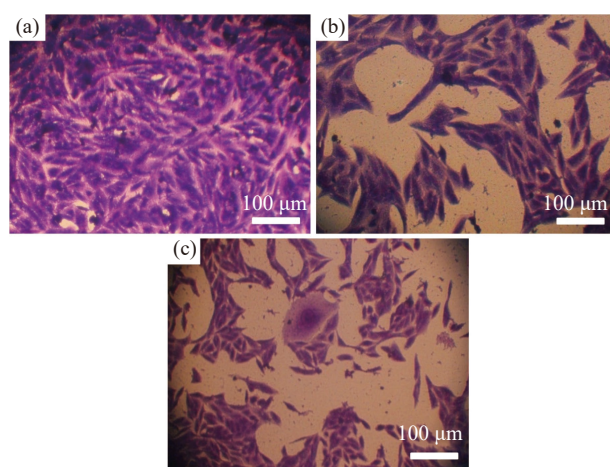


Fig. 7 Morphological changes in MCF-7 cancerous cells upon incubation with selenium NPs prepared by using chemical reduction of sodium selenite with ascorbic acid as a reducing agent in the presence of vitamin E TPGS as a stabilizing agent, where SeNPs were encapsulated individually with both of PLGA NPs and PLGA-FA NPs for 24 h at 37 °C. (a) Untreated MCF-7 cells as a control sample. (b) MCF7 cells treated with Se-TPGS-PLGA. (c) MCF7 cells treated with Se-TPGS-PLGA-PEG-FA.

Apoptosis study by AO/EtBr dual staining method

This assay was applied as a method to inspect the occurrence of apoptosis process that induced in MCF-7 cell line when exposing them to synthesized Se-TPGS-PLGA and Se-TPGS-PLGA-PEG-FA. AO is a fluorescent cationic dye, pervades the plasma membrane of cells and binds to nucleic acids to emit green fluorescence when bound to double strand DNA (dsDNA), and emits red fluorescence when bound to single strand (ssDNA) or RNA. This unique characteristic makes acridine orange useful for cell-cycle studies. AO has also been used as a

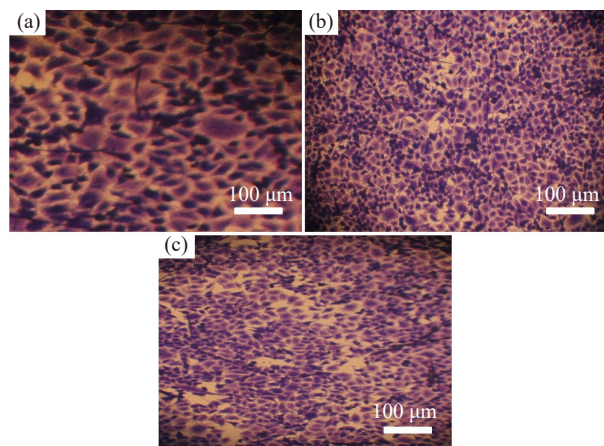


Fig. 8 Morphological changes in HBL cells upon incubation with selenium NPs prepared by using chemical reduction of sodium selenite with ascorbic acid as a reducing agent in the presence of vitamin E TPGS as a stabilizing agent, where SeNPs were encapsulated individually with both of PLGA NPs and PLGA-FA NPs for 24 h at 37 °C. (a) Untreated HBL cells as a control sample. (b) HBL cells treated with Se-TPGS-PLGA NPs. (c) HBL cells treated with Se-TPGS-PLGA-PEG-FA NPs.

lysosomal dye when examined under a fluorescent light microscope. Ethidium bromide stain is a permeable for dead cells, i.e., when cell membrane integrity is damaged, and binds to dsDNA to emit orange fluorescence [50]. Analysis of AO/EtBr staining demonstrated that the synthetic polymeric nanoformulations prompted apoptosis in MCF-7 cells as stated Figs. 9(b) and 9(c), in comparison with untreated cells (Figs. 9(a) and 9(b)).

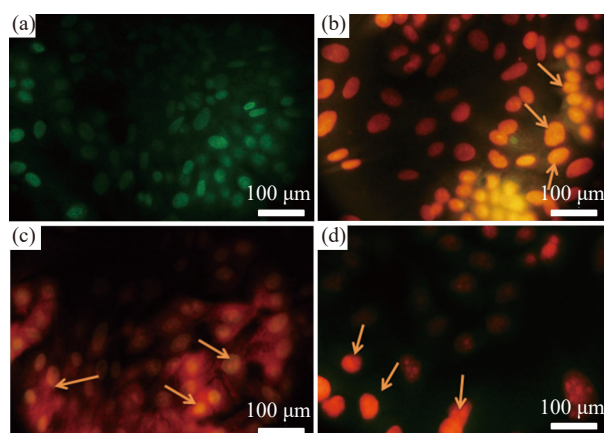


Fig. 9 Fluorescence images of MCF-7 cells stained with AO/EtBr cell viability assay after incubation for 24 h with selenium NPs prepared by using chemical reduction of sodium selenite with ascorbic acid as a reducing agent in the presence of vitamin E TPGS as a stabilizing agent, where SeNPs-vitamin E TPGS was encapsulated individually with both of PLGA NPs and PLGA-FA NPs for 24 h at 37 °C. (a) and (b) Untreated MCF7 cells as a control sample. (c) MCF7 cells treated with Se-TPGS-PLGA NPs. (d) MCF7 cells treated with Se-TPGS-PLGA-PEG-FA NPs.

Antioxidant Potential Evaluation by DPPH Assay

The antioxidant activity of Se-TPGS-PLGA and Se-TPGS-PLGA-FA nanoformulation was examined by using a colorimetric DPPH assay. The DPPH radical-scavenging (%) activities exhibited strong antioxidant activity as depicted in Fig. 10. This activity is attributed to the synergistic effect of both antioxidant activity for selenium and vitamin E TPGS. In general, SeNPs promote the growth of animals, and they can act as antibacterial agents and antioxidants and improve the immune system [51]. Nano antioxidants are emerging as a new technique for antioxidant therapy to cure and/or prevent illnesses involving oxidative stress, primarily those generated from materials with biological antioxidant potentials such as selenium and vitamins, primarily vitamin E in their composition. Because of their size and high surface area, NPs have more powerful interactions with molecules in biological systems, making them more effective antioxidants against free radical damage than small molecules. This work outlines a straightforward method for synthesizing SeNPs [52].

Hemocompatibility assessment

The interaction (hemolytic potential) of RBCs *in vitro* is one of the most basic tests used to determine the safety of blood-contacting medical materials. Blood is a complicated tissue made up of 55% plasma, 44% red blood cells, and 1% leukocytes and platelets. RBCs are biconcave discoid cells that contain hemoglobin as an oxygen carrier [53]. Hemolysis is defined as the destruction of RBCs that results in the release of the iron-containing protein hemoglobin into the bloodstream, resulting in anemia, jaundice, renal toxicity, and other related pathological conditions [54]. This test is strongly recommended for integrating preclinical test procedures preceding the *in vivo* application of new nanoformulation therapies [55]. Therefore, it is vital to investigate influence of the encapsulated formulas Se-TPGS-PLGA and Se-TPGS-PLGA-PEG-FA on human red blood cells. Hemolysis studies were carried out on these formulations for the blood samples and examined RBCs visually and by using a fluorescence microscopy as explained in Figs. 11(b) and 11(c), compared with the untreated RBCs in Fig. 11(a).

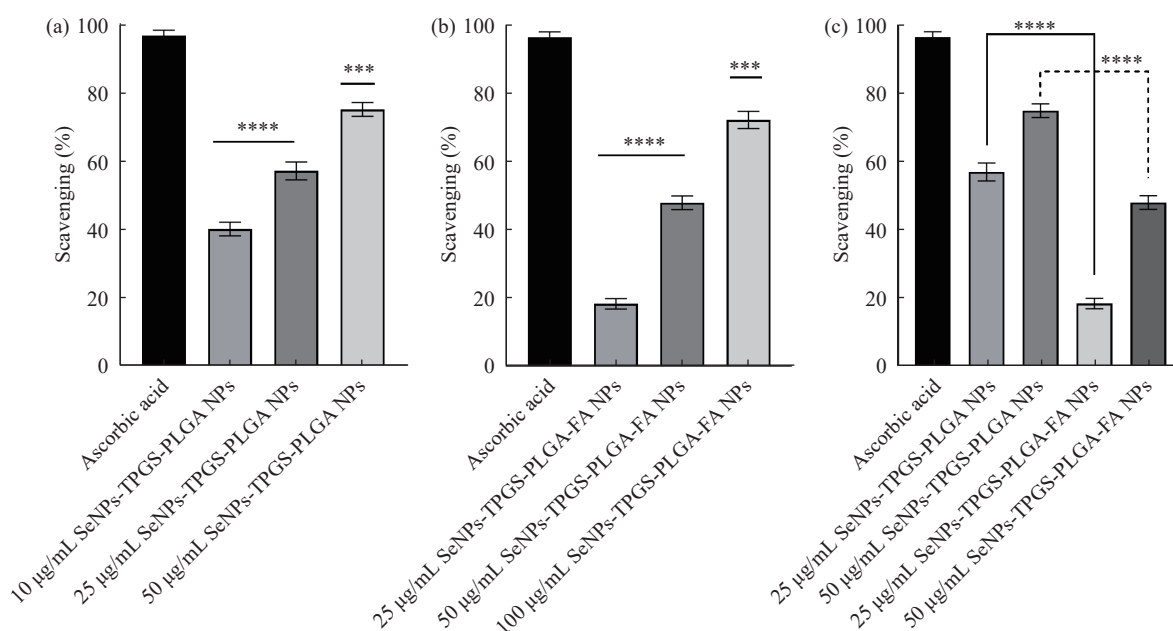


Fig. 10 Antioxidant activity by DPPH assay for selenium NPs prepared by using chemical reduction of sodium selenite with ascorbic acid as a reducing agent in the presence of vitamin E TPGS as a stabilizing agent, where SeNPs were encapsulated individually with both of PLGA NPs and PLGA-FA NPs. (a) Antioxidant activity of Se-TPGS-PLGA NPs. (b) Antioxidant activity of Se-TPGS-PLGA-PEG-FA NPs. (c) Statistical comparison between 25 and 50 µg/mL of Se-TPGS-PLGA NPs and 25 and 50 µg/mL of Se-TPGS-PLGA-FA NPs. All results were performed in triplicate and repeated three times and achieved statistically using GraphPad Prism 8.0 where non-significant (ns) $P > 0.05$, $*P \leq 0.05$, $**P \leq 0.01$, $***P \leq 0.001$, and $****P \leq 0.0001$.

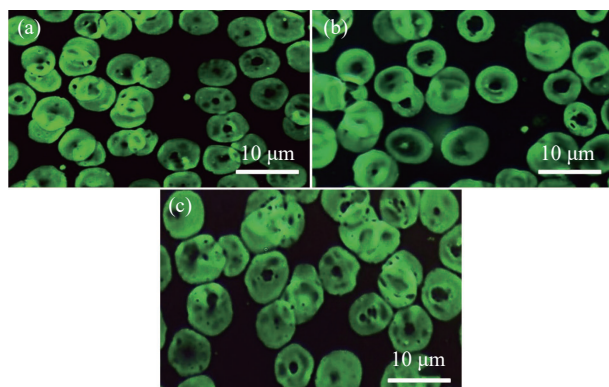


Fig. 11 Hemolysis assay of RBC incubated with SeNPs prepared by using chemical reduction of sodium selenite with ascorbic acid as a reducing agent in the presence of vitamin E TPGS as a stabilizing agent, then SeNPs were encapsulated individually with both of PLGA NPs and PLGA-FA NPs. **(a)** normal saline solution as a control sample of RBC, **(b)** RBC after incubation with SeNPs-TPGS-PLGA, and **(c)** RBC after incubation with SeNPs-TPGS-PLGA-PEG-FA.

Conclusion

The novel hybrid drug delivery system for the encapsulation of vitamin E TPGS stabilized selenium NPs into PLGA polymers was synthesized using oil in water (o/w) emulsion evaporation technique using polyvinyl alcohol as a surfactant. The synthesized nanoformulations were nano-sized scale with spherical shape. Additionally, it can be proposed that encapsulation SeNPs with PLGA-PEG-FA appears significantly promising results for targeting cancer cells with a folate positive receptor, causing synergistic inhibitory effect between selenium and vitamin E against MCF-7 breast cancer cells. However, it showed no significant effect on the normal HBL cell line. Furthermore, these formulations have appeared sustained release with anticancer activity against MCF-7 cells with minimum side effect on human normal cells as well as substantial antioxidant activity and interesting nonhemolytic effect.

CRedit Author Statement

Haider Hamzah Al-Shreefy: Conceptualization, Methodology, Validation, Data curation, Writing – original draft, Investigation, Resources, Software. **Estabraq Al-Wasiti:** Supervision, Project administration, Funding acquisition. **Mohammed J. Al-Awady:** Formal analysis, Writing–review & editing, Software, Supervision, Funding acquisition.

Conflict of Interest

The authors declare that no competing interest exists.

References

- [1] S. Bhatia, T. Naved, S. Sardana. Introduction to Pharmaceutical Biotechnology, Volume 3: Animal tissue culture and biopharmaceuticals. IOP Publishing Ltd., 2019.
- [2] S.S. Feng, S. Chong, J. Rompas. Chemotherapeutic Engineering: Collected Papers of Si-Shen Feng-a Tribute to Shu Chien on His 82nd Birthday. Hoboken: Pan Stanford, 2014.
- [3] Z. Zhang, P.C. Tsai, T. Ramezanli, et al. Polymeric nanoparticles-based topical delivery systems for the treatment of dermatological diseases. *Nanomedicine and Nanobiotechnology*, 2013, 5(3): 205–218. <https://doi.org/10.1002/wnan.1211>
- [4] A.M. Grumezescu. Multifunctional Systems for Combined Delivery, Biosensing and Diagnostics. William Andrew, 2017.
- [5] N. Al-Janabi, M. Al-Awady. Antibacterial activity of graphene oxide nanosheet against salmonella associated food contamination. *Eurasian Scientific Herald*, 2021, 3: 44–51.
- [6] W.H. Mohammed, W.K. Ali, M.J. Al-Awady. Evaluation of *in vitro* drug release kinetics and antibacterial activity of vancomycin HCl-loaded nanogel for topical application. *Journal of Pharmaceutical Science and Research*, 2018, 10(11): 2747–2756.
- [7] J.K. Patra, G. Das, L.F. Fraceto, et al. Nano based drug delivery systems: Recent developments and future prospects. *Journal of Nanobiotechnology*, 2018, 16(1): 71. <https://doi.org/10.1186/s12951-018-0392-8>
- [8] J.L. Arias. Nanotechnology and Drug Delivery, Volume Two: Nano-Engineering Strategies and Nanomedicines against Severe Diseases. CRC Press, 2016.
- [9] S. Sharma, A. Parmar, S. Kori, et al. PLGA-based nanoparticles: A new paradigm in biomedical applications. *TrAC Trends in Analytical Chemistry*, 2016, 80: 30–40. <https://doi.org/10.1016/j.trac.2015.06.014>
- [10] F.P. Kratz, H. Senter. Steinhagen. Drug delivery in oncology: from basic research to cancer therapy. John Wiley & Sons, 2013.
- [11] A.K. Mitra, K. Cholkar, A. Mandal. Emerging Nanotechnologies for Diagnostics, Drug Delivery and Medical Devices. William Andrew, 2017.
- [12] P. Mishra, B. Nayak, R.K. Dey. PEGylation in anti-cancer therapy: An overview. *Asian Journal of Pharmaceutical Sciences*, 2016, 11(3): 337–348. <https://doi.org/10.1016/j.ajps.2015.08.011>
- [13] N. Raina, A.K. Singh, A. Islam. Biological implications of polyethylene glycol and PEGylation: therapeutic approaches based on biophysical studies and protein structure-based drug design tools. In: Innovations and Implementations of Computer Aided Drug Discovery Strategies in Rational Drug Design. Springer, 2021: 273–294.
- [14] W.S. Saw, T. Anasamy, Y.Y. Foo, et al. Delivery of nanoconstructs in cancer therapy: challenges and therapeutic opportunities. *Advanced Therapeutics*, 2021, 4(3): 2000206. <https://doi.org/10.1002/adtp.202000206>
- [15] L. Zerrillo, K.B.S.S. Gupta, F.A.W.M. Lefeber, et al. Novel fluorinated poly (lactic-Co-glycolic acid) (PLGA) and polyethylene glycol (PEG) nanoparticles for

- monitoring and imaging in osteoarthritis. *Pharmaceutics*, 2021, 13(2): 235. <https://doi.org/10.3390/pharmaceutics13020235>
- [16] J.O. Morales, P.J. Gaillard. *Nanomedicines for Brain Drug Delivery*. Springer, 2021.
- [17] S. Jahan, M.E. Karim, E.H. Chowdhury. Nanoparticles targeting receptors on breast cancer for efficient delivery of chemotherapeutics. *Biomedicines*, 2021, 9(2): 114. <https://doi.org/10.3390/biomedicines9020114>
- [18] R. Vivek, C. Rejeeth, R. Thangam. Targeted Nanotherapeutics based on cancer biomarkers, in Multifunctional Systems for Combined Delivery, Biosensing and Diagnostics. Elsevier, 2017: 229–244.
- [19] X.L. Huo, Y.Q. Zhang, X.C. Jin, et al. A novel synthesis of selenium nanoparticles encapsulated PLGA nanospheres with curcumin molecules for the inhibition of amyloid β aggregation in Alzheimer's disease. *Journal of Photochemistry and Photobiology B, Biology*, 2019, 190: 98–102. <https://doi.org/10.1016/j.jphotobiol.2018.11.008>
- [20] C.A. Gutiérrez-Valenzuela, P. Guerrero-Germán, A. Tejada-Mansir, et al. Folate functionalized PLGA nanoparticles loaded with plasmid pVAX1-NH36: Mathematical analysis of release. *Applied Sciences*, 2016, 6(12): 364. <https://doi.org/10.3390/app6120364>
- [21] K.S. Khashan, G.M. Sulaiman, S.A. Hussain, et al. Synthesis, characterization and evaluation of antibacterial, anti-parasitic and anti-cancer activities of aluminum-doped zinc oxide nanoparticles. *Journal of Inorganic and Organometallic Polymers and Materials*, 2020, 30(9): 3677–3693. <https://doi.org/10.1007/s10904-020-01522-9>
- [22] Z. Ali, M. Jabir, A. Al-Shammari. Gold nanoparticles inhibiting proliferation of Human breast cancer cell line. *Research Journal of Biotechnology*, 2019, 14: 79–82.
- [23] A.G. Al-Ziyadi, A.M. Al-Shammari, M.I. Hamzah, et al. Newcastle disease virus suppress glycolysis pathway and induce breast cancer cells death. *Virusdisease*, 2020, 31(3): 341–348. <https://doi.org/10.1007/s13337-020-00612-z>
- [24] M.J. Al-Awady, A.A. Balakit, A. Al-Musawi, et al. Investigation of anti-MRSA and anticancer activity of eco-friendly synthesized silver nanoparticles from palm dates extract. *Nano Biomedicine and Engineering*, 2019, 11(2): 157–169. <https://doi.org/10.5101/nbe.v11i2.p157-169>
- [25] K.S. Khashan, M.S. Jabir, F.A. Abdulameer. Carbon Nanoparticles prepared by laser ablation in liquid environment. *Surface Review and Letters*, 2019, 26(10): 1950078. <https://doi.org/10.1142/S0218625X19500781>
- [26] C. Networking. *Manual of Immunological Methods*. Boca Raton: CRC Press, 1998.
- [27] D. Sunil, P. Kamath, H.R. Chandrashekhar. *In Vitro Bioassay Techniques for Anticancer Drug Discovery and Development*. Boca Raton: CRC Press, 2017.
- [28] S. Boroumand, M. Safari, E. Shaabani, et al. Selenium nanoparticles: synthesis, characterization and study of their cytotoxicity, antioxidant and antibacterial activity. *Material Research Express*, 2019, 6(8): 0850d8. <https://doi.org/10.1088/2053-1591/ab2558>
- [29] M.S. Jabir, A.A. Taha, U.I. Sahib, et al. Novel of nano delivery system for Linalool loaded on gold nanoparticles conjugated with CALNN peptide for application in drug uptake and induction of cell death on breast cancer cell line. *Materials Science & Engineering C, Materials for Biological Applications*, 2019, 94: 949–964. <https://doi.org/10.1016/j.msec.2018.10.014>
- [30] L.N. Zhou, Z.T. Song, S.J. Zhang, et al. Construction and antitumor activity of selenium nanoparticles decorated with the polysaccharide extracted from Citrus Limon (L.) Burm. f. (Rutaceae). *International Journal of Biological Macromolecules*, 2021, 188: 904–913. <https://doi.org/10.1016/j.ijbiomac.2021.07.142>
- [31] J. Condé. *Handbook of Nanomaterials for Cancer Theranostics*. Elsevier, 2018.
- [32] H.M. Aldawsari, U.A. Fahmy, F. Abd-Allah, et al. Formulation and optimization of avanafil biodegradable polymeric nanoparticles: A single-dose clinical pharmacokinetic evaluation. *Pharmaceutics*, 2020, 12(6): 596. <https://doi.org/10.3390/pharmaceutics12060596>
- [33] M. Kaszuba, D. McKnight, M.T. Connah, et al. Measuring sub nanometre sizes using dynamic light scattering. *Journal of Nanoparticle Research*, 2008, 10(5): 823–829. <https://doi.org/10.1007/s11051-007-9317-4>
- [34] M.R. Singh. *Advances and Avenues in the Development of Novel Carriers for Bioactives*. London: Academic Press, 2020.
- [35] D. Fikai, A.M. Grumezescu. *Nanostructures for Novel Therapy: Synthesis, Characterization and Applications*. Elsevier, 2017.
- [36] K.K. Jain. Drug delivery systems - An overview. In: *Drug Delivery Systems. Methods in Molecular Biology™*, vol 437. Humana Press, 2008. https://doi.org/10.1007/978-1-59745-210-6_1
- [37] R. Prasad, A.K. Jha, K. Prasad. *Exploring the Realms of Nature for Nanosynthesis*. Springer, 2018.
- [38] C.E. Astete, D. Dolliver, M. Whaley, et al. Antioxidant poly(lactic-co-glycolic) acid nanoparticles made with α -tocopherol-ascorbic acid surfactant. *ACS Nano*, 2011, 5(12): 9313–9325. <https://doi.org/10.1021/nn102845t>
- [39] S. Acharya, S.K. Sahoo. PLGA nanoparticles containing various anticancer agents and tumour delivery by EPR effect. *Advanced Drug Delivery Reviews*, 2011, 63(3): 170–183. <https://doi.org/10.1016/j.addr.2010.10.008>
- [40] G. Midekessa, K. Godakumara, J. Ord, et al. Zeta potential of extracellular vesicles: Toward understanding the attributes that determine colloidal stability. *ACS Omega*, 2020, 5(27): 16701–16710. <https://doi.org/10.1021/acsomega.0c01582>
- [41] S.S. Mohapatra, S. Ranjan, N. Dasgupta, et al. *Characterization and Biology of Nanomaterials for Drug Delivery: Nanoscience and Nanotechnology in Drug Delivery*. Elsevier, 2018. <https://doi.org/10.1016/C2017-0-00272-0>
- [42] P. Rai, S.A. Morris. *Nanotheranostics for Cancer Applications*. Springer, Cham, 2019. <https://doi.org/10.1007/978-3-030-01775-0>
- [43] E. Piacenza, A. Presentato, F. Ferrante, et al. Biogenic selenium nanoparticles: A fine characterization to unveil their thermodynamic stability. *Nanomaterials*, 2021, 11(5): 1195. <https://doi.org/10.3390/nano11051195>
- [44] E. Assadpour, H. Rostamabadi, S.M. Jafari. Introduction to characterization of nanoencapsulated food ingredients. In: *Characterization of Nanoencapsulated Food Ingredients*. Elsevier, 2020: 1–50.
- [45] W. Huang, C. Zhang. Tuning the size of poly (lactic-co-glycolic acid) (PLGA) nanoparticles fabricated by nanoprecipitation. *Biotechnology Journal*, 2018, 13(1): 1700203. <https://doi.org/10.1002/biot.201700203>
- [46] A. Zielińska, F. Carreiró, A.M. Oliveira, et al. Polymeric nanoparticles: Production, characterization, toxicology and ecotoxicology. *Molecules*, 2020, 25(16): E3731. <https://doi.org/10.3390/molecules25163731>
- [47] W. Jiang, Y. Fu, F. Yang, et al. Gracilaria lemaneiformis polysaccharide as integrin-targeting surface decorator of selenium nanoparticles to achieve enhanced anticancer efficacy. *ACS Applied Materials & Interfaces*, 6(16): 13738–13748. <https://doi.org/10.1021/am5031962>
- [48] D. Li, S. Liu, J. Zhu, et al. Folic acid modified TPGS as a novel nano-micelle for delivery of nitidine chloride to

- improve apoptosis induction in Huh7 human hepatocellular carcinoma. *BMC Pharmacology & Toxicology*, 2021, 22(1): 1. <https://doi.org/10.1186/s40360-020-00461-y>
- [49] A.R. Shahverdi, F. Shahverdi, E. Faghfuri, et al. Characterization of folic acid surface-coated selenium nanoparticles and corresponding *in vitro* and *in vivo* effects against breast cancer. *Archives of Medical Research*, 2018, 49(1): 10–17. <https://doi.org/10.1016/j.arcmed.2018.04.007>
- [50] J.J. Marizcurrena, M.F. Cerdá, D. Alem, et al. Living with pigments: The colour palette of antarctic life. In: *The Ecological Role of Micro-organisms in the Antarctic Environment*. Springer, 2019. https://doi.org/10.1007/978-3-030-02786-5_4
- [51] A.S. Kassim, A.H.H. Ali, T.A. Marwan, et al. Selenium nanoparticles in rabbit nutrition: a review. *SVU-International Journal of Agricultural Sciences*, 2022, 4(1): 90–98. <https://doi.org/10.21608/svuijas.2022.117298.1171>
- [52] W. Zhang, J. Zhang, D. Ding, et al. Synthesis and antioxidant properties of Lycium barbarum polysaccharides capped selenium nanoparticles using tea extract. *Artificial Cells, Nanomedicine, and Biotechnology*, 2018, 46(7): 1463–1470. <https://doi.org/10.1080/21691401.2017.1373657>
- [53] R.P. Rother, L. Bell, P. Hillmen, et al. The clinical sequelae of intravascular hemolysis and extracellular plasma hemoglobin: a novel mechanism of human disease. *JAMA*, 2005, 293(13): 1653–1662. <https://doi.org/10.1001/jama.293.13.1653>
- [54] S. Siddiquee, M.G.J. Hong, M.M. Rahman. *Composite materials: applications in engineering, biomedicine and food science*. Springer, 2020. <https://doi.org/10.1007/978-3-030-45489-0>
- [55] S. Krajewski, R. Prucek, A. Panacek, et al. Hemocompatibility evaluation of different silver nanoparticle concentrations employing a modified Chandler-loop *in vitro* assay on human blood. *Acta Biomaterialia*, 2013, 9(7): 7460–7468. <https://doi.org/10.1016/j.actbio.2013.03.016>

© The author(s) 2023. This is an open-access article distributed under the terms of the Creative Commons Attribution 4.0 International License (CC BY) (<http://creativecommons.org/licenses/by/4.0/>), which permits unrestricted use, distribution, and reproduction in any medium, provided the original author and source are credited.